Real-time MRI-guided right heart catheterization in adults using passive catheters

Kanishka Ratnayaka[1,2], Anthony Z. Faranesh[1], Michael S. Hansen[1], Annette M. Stine[1], Majdi Halabi[1], Israel M. Barbash[1], William H. Schenke[1], Victor J. Wright[1], Laurie P. Grant[1], Peter Kellman[1], Ozgur Kocaturk[1], and Robert J. Lederman[1]*

[1]Division of Intramural Research, Cardiovascular and Pulmonary Branch, National Heart Lung and Blood Institute, National Institutes of Health, Building 10, Room 2c713, MSC 1538, Bethesda, MD 20892-1538, USA; and [2]Department of Cardiology, Children's National Medical Center, Washington, DC, USA

Aims	Real-time MRI creates images with superb tissue contrast that may enable radiation-free catheterization. Simple procedures are the first step towards novel interventional procedures. We aim to perform comprehensive transfemoral diagnostic right heart catheterization in an unselected cohort of patients entirely using MRI guidance.
Methods and results	We performed X-ray and MRI-guided transfemoral right heart catheterization in consecutive patients undergoing clinical cardiac catheterization. We sampled both cavae and both pulmonary arteries. We compared success rate, time to perform key steps, and catheter visibility among X-ray and MRI procedures using air-filled or gadolinium-filled balloon-tipped catheters. Sixteen subjects (four with shunt, nine with coronary artery disease, three with other) underwent paired X-ray and MRI catheterization. Complete guidewire-free catheterization was possible in 15 of 16 under both. MRI using gadolinium-filled balloons was at least as successful as X-ray in all procedure steps, more successful than MRI using air-filled balloons, and better than both in entering the left pulmonary artery. Total catheterization time and individual procedure steps required approximately the same amount of time irrespective of image guidance modality. Catheter conspicuity was best under X-ray and next-best using gadolinium-filled MRI balloons.
Conclusion	In this early experience, comprehensive transfemoral right heart catheterization appears feasible using only MRI for imaging guidance. Gadolinium-filled balloon catheters were more conspicuous than air-filled ones. Further workflow and device enhancement are necessary for clinical adoption.
Keywords	Catheterization • Magnetic resonance imaging • Interventional cardiovascular MRI • Pulmonary artery

Introduction

Ionizing radiation to guide cardiac catheterization is unattractive especially in paediatrics applications and prolonged procedures. Exposure to X-rays is reduced only partially by meticulous technique and adjunctive imaging guidance. Real-time magnetic resonance imaging (MRI) could provide a radiation-free alternative to X-ray guidance of cardiac catheterization, and depicts blood and soft tissue in any orientation.[1]

As a first step towards more advanced MRI catheterization procedures, we performed investigational MRI-guided transfemoral right heart catheterization in an unselected cohort of adults undergoing X-ray heart catheterization. In this pilot study, we compared X-ray and MRI performance times in comprehensive catheterization. We tested the hypotheses that: (i) MRI right heart catheterization can be performed safely using passive balloon catheters even in patients traditionally considered 'difficult' because, for example, of dilated heart structures or elevated pulmonary artery pressures; (ii) Gadolinium-filled balloons are more conspicuous and therefore more effective than air-filled balloons for MRI catheterization; (iii) MRI catheterization procedure times are comparable with X-ray procedure times, yet require no radiation. This is the first paired comparison of X-ray and MRI catheterization.

Methods

Study design

The protocol was approved by the Institutional Review Board (NCT01287026), and was performed at the NIH Clinical Center in Bethesda, MD. The authors have direct custody of all data.

Consecutive adults undergoing urgent or elective left heart catheterization were invited to participate, even if right heart catheterization was not indicated. Subjects consented in writing but were excluded for cardiovascular instability (including ST-elevation myocardial infarction, refractory angina, or refractory heart failure), pregnancy or nursing, an estimated glomerular filtration rate <30 mL/min/ 1.73 m^2 (in case a gadolinium-balloon were to rupture), or ineligibility for MRI.

We chose a transfemoral route because of compatibility with our laboratory workflow and because it requires imaging guidance. All right heart catheterizations included chamber sampling for pressure and oximetry, and timed performance of specific steps (see Section 'Performance measures and data analysis').

After the clinical X-ray catheterization was completed using moderate sedation, all subjects verbally reiterated willingness to proceed. The femoral vein was accessed for X-ray and MRI catheterization if not already accessed. Next, subjects were transferred into an adjoining 1.5T MRI system (Espree, Siemens Medical Solutions, Erlangen, Germany) using a dedicated intermodality transfer table (Miyabi, Siemens), while maintaining sterility of the operating field (Figure 1).[1] The suite is equipped with an investigational real-time MRI

acquisition-and-display console (Interactive Front End, Siemens Corporate Research, Princeton NJ, USA) having NHLBI enhancements (such as interactive slice thickness adjustment and interactive saturation-mode to enhance the contrast of gadolinium-contrast);[2] in-room LCD projectors; a custom six-lead surface ECG interface to a commercial haemodynamics recording system[3] that also displays invasive blood pressure and non-invasive haemoglobin saturation; and 'open-microphone' acoustic noise-cancelling MRI headsets for staff and patient (IMROC, Opto-acoustics, Moshav Mazor, Israel).

Magnetic resonance imaging localizers were obtained at abdominal and cardiac 'stations' to allow catheters to be visualized as they were advanced from the groin to the heart. Cardiac function was assessed using a highly accelerated 'mini exam' using parallel imaging (TGRAPPA rate 4), to acquire a stack of short-axis slices covering the heart during free breathing, with a temporal resolution of 59 ms.[4] Typical imaging parameters were balanced steady-state free precession (SSFP) with fractional echos; TR/TE, 2.6/1.1 ms; flip angle, 50°; bandwidth, 1085 Hz per pixel; matrix, 192 × 92; slice thickness, 6 mm, and GRAPPA rate 4. Task-specific slice prescriptions were saved to facilitate different procedure stages (bi-caval, right ventricular outflow tract, and pulmonary artery bifurcation) (Supplementary material online, Figure). Typical real-time MRI parameters were SSFP; TR/TE, 2.88/1.44 ms; flip angle, 40°; bandwidth, 1000 Hz per pixel; matrix 192 × 144; FOV, 35 × 35 cm; slice thickness, 6 mm; and GRAPPA rate 1−2, with a temporal resolution up to 150 ms (7 frames/s).

Transfemoral right heart catheterization was performed first under X-ray and then twice under continuous real-time MRI guidance using
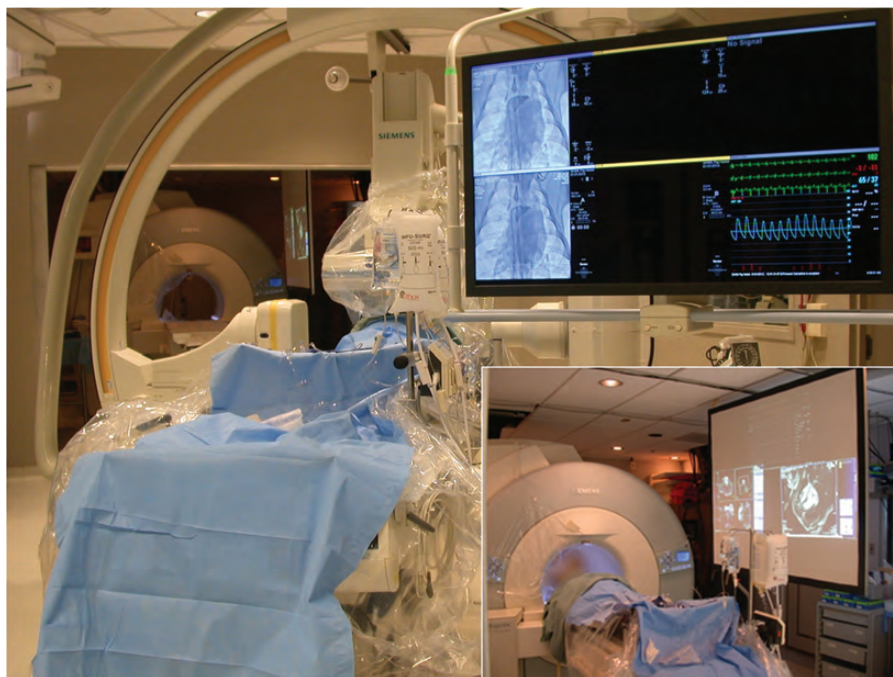

Figure 1 A combined X-ray and magnetic resonance imaging intervention suite. Adjoining independent X-ray and magnetic resonance imaging systems are separated by radiofrequency- and X-ray-shielded doors. The X-ray system table is mounted on motorized rails. When the doors are opened and the X-ray gantries parked, the X-ray and magnetic resonance imaging tables can dock, and the patient can be transferred smoothly and rapidly between systems. *Inset*: the magnetic resonance imaging system is configured like an X-ray interventional system. Multiple LCD projectors display real-time magnetic resonance imaging, scanner control, and the same haemodynamic recording system as X-ray.

balloon wedge end-hole catheters (7 Fr Arrow-Teleflex, Limerick, PA) filled in random order with air or with 2% diluted gadolinium (gadopentetate-dimeglumine, Magnevist 0.1 mM, Bayer Healthcare, Tarrytown, NY, USA). Additional sedation was administered as needed.

Procedures were performed by attending physicians with at least 5 years of experience in adult or paediatric interventional cardiology.

Performance measures and data analysis

Four specific procedure steps were used as performance measures: entry of superior vena cava from right atrium, main pulmonary artery from right ventricle, and each branch pulmonary artery from main pulmonary artery. Success or failure to enter without a guidewire was recorded, as was time required for each step. To minimize research-related radiation exposure, guidewire-free attempts were aborted under X-ray after 2 min, after which a guidewire was employed for selective engagement. Because no MRI-safe guidewires are available at present, no guidewires were used under MRI. Total catheterization times reflect intervals between pulmonary artery catheters first entering and then exiting the body, and includes catheter manipulation and sampling pressure and oximetry.

Image-guidance was assessed on two ordinal scales. Confidence in the position of the catheter was graded as uncertain, probable but needing pressure confirmation, or certain. Conspicuity of catheter was rated as tip sometimes visible but sometimes not located easily; tip visible most times but located easily; tip visible at all times; or tip plus shaft visible at all times. The conspicuity scale was intrinsically biased in favour of X-ray in this protocol.

Magnetic resonance images were analysed on a dedicated workstation (Argus, Siemens). Data were analysed using PASW Statistics v19 (SPSS/IBM, Armonk, NY) and Prism v5.3 (Graphpad Software, La Jolla, CA, USA). Data are expressed as mean $\pm$ standard deviation, except for time to perform procedure steps, which are expressed as median (inter-quartile range). Success among approaches was analysed using a Cochran Q test and then pairwise *post hoc* using a related samples McNemar test. Success rates and performance times were compared among procedures. These were not normally distributed and therefore were analysed using a Friedman χ^2 test and then pairwise *post hoc* using a two-tailed Wilcoxon signed rank test. A secondary analysis censored steps requiring >120 s, reclassifying them as unsuccessful. Missing data were not imputed. A two-tailed $P < 0.05$ was considered significant except for pairwise *post hoc* comparisons (e.g. our planned test of MRI air vs. MRI gadolinium) in which a more conservative $P < 0.025$ was considered significant.

Results

Subjects

Twenty-three consecutive patients were invited to participate, of whom two were ineligible, three declined, and 18 consented. Of these, two were unstable after the clinical catheterization procedure but before MRI (one with severe biventricular and respiratory failure, the other with persistent angina before cardiac surgery) and were excluded. Of the remaining 16 subjects, indications were shunt in four (atrial septal defect in three, coronary arteriovenous fistula in one); coronary artery disease in nine (three undergoing PCI and one undergoing endomyocardial biopsy during the same session); other in three (effusive-constrictive pericardial disease, chronic thromboembolic pulmonary hypertension, and rheumatic mitral and prosthetic aortic disease, respectively). Right heart

catheterization was not indicated in 5 of these 16 subjects. Demographics are described in *Table 1*.

Total fluoroscopy time was 11.8 ± 6.1 min, of which 5.1 ± 2.1 min were used for right heart catheterization, and the remainder for diagnostic or interventional left heart procedures. The corresponding radiation dose-area-product for right heart catheterization was 22.5 ± 34.8 mGy cm^2.

Safety

Complete MRI catheterization was unsuccessful in only one subject (subject #04) who had a large secundum atrial septal defect with large pulmonary arteries and moderate pulmonary artery hypertension (ratio of pulmonary artery to aortic pressure, 0.4). In this subject, both X-ray and MRI pulmonary artery catheterization failed without a guidewire. No guidewire is currently available for use under MRI; a guidewire could be used only under X-ray.

In two patients, only one of two sequential MRI catheterizations was performed. One requested exit from the MRI because of hunger and dyspnoea. In another the catheter shaft was suspected to be kinked during the second MRI catheterization; it was withdrawn uneventfully but not reintroduced. One other patient had a suspected catheter kink after successful completion of both MRI catheterizations; it too was removed by simple withdrawal. Both catheter kinks were recognized immediately based on altered tactile feedback and on paradoxical tip retraction during catheter advancement.

One subject had transient pulse oximetry desaturation attributed to moderate sedation, corrected with repositioning to open the airway. Otherwise moderate sedation was conducted as during X-ray procedures. When needed, a language interpreter seated in the control room assisted in communications. There were no other research-related adverse events.

Table 1 Demographic characteristics of research subjects

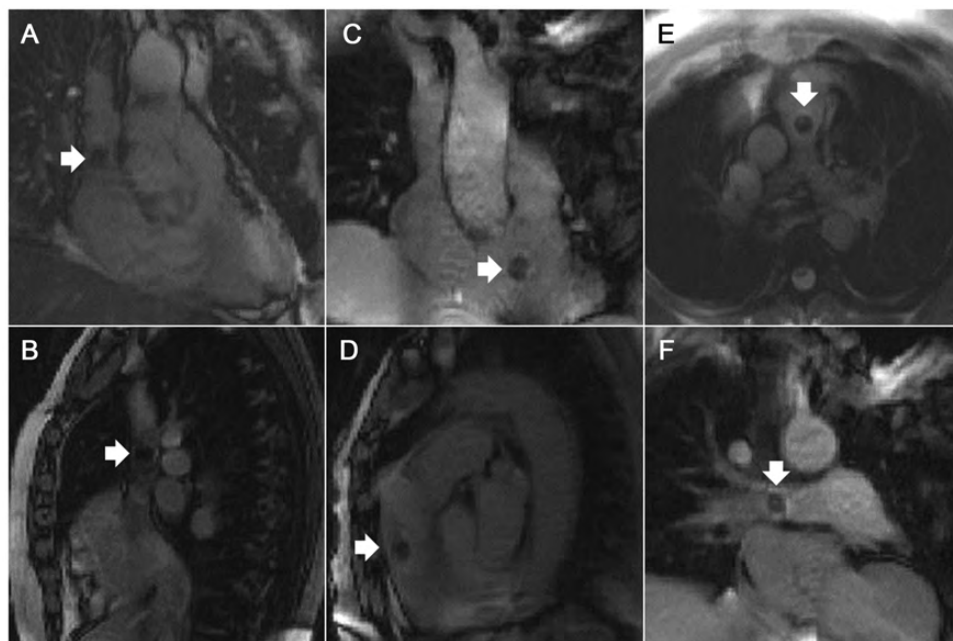| Characteristic	Finding
Age	60.5 ± 12.5
Gender	44% female
Language	69% non-English
Height	160.4 ± 10.2 cm
Weight	71.0 ± 15.5 kg
Hypertension (%)	81
Diabetes mellitus (%)	31
Tobacco prior or current (%)	13
Coronary artery disease (%)	50
Reduced LV systolic function (%)	25
Congestive heart failure (%)	25
Congenital heart disease (%)	19
Prior cardiac surgery (%)	13
Atrial fibrillation (%)	13
Malignancy (%)	6

Figure 2 Magnetic resonance imaging catheterization using an air-filled balloon catheter. White arrows indicate catheter tips. Panels depict different chambers. (*A* and *B*) Superior vena cava. (*C* and *D*) Entering the main pulmonary artery from the right ventricle. (*E*) Main pulmonary artery bifurcation. (*F*) Right pulmonary artery.

Magnetic resonance imaging catheterization findings

Real-time MRI allowed continuous visualization of transfemoral catheterization during navigation into all selected vessels and chambers. *Figure 2* shows typical still frames of MRI catheterization using an air-filled balloon catheter. *Figure 3* shows typical images of MRI catheterization using a gadolinium-filled balloon catheter. 'Saturation preparation' mode could be turned on interactively to enhance the appearance of gadolinium-filled, but not air-filled, balloons (Supplementary material online, *Video*).

There were no important clinical differences between pressure measurements or between haemoglobin oximetry measurements obtained among approaches (*Table 2*). Three-quarters of subjects had pulmonary artery pressures exceeding 35 mmHg. The average ratio of the pulmonary artery to the aorta was 0.31 ± 0.09; it exceeded 0.4 in three of 16 subjects.

Success rates were similar for chamber-entry tasks, whether X-ray using air-filled balloon catheters or MRI using air- or gadolinium-filled balloon catheters (*Table 3*). Magnetic resonance imaging using gadolinium-filled balloons was always at least as successful as X-ray. After censoring comparisons of steps requiring >120 s, the results were essentially unchanged (data not shown).

Different procedure steps required approximately the same amount of time irrespective of image-guidance modality (*Table 4*). In entering the left pulmonary artery from the main pulmonary artery, there were trends for MRI with gadolinium-filled catheters to navigate faster than X-ray or MRI with air-filled MRI catheters. The results were essentially unchanged after censoring comparisons of steps requiring >120 s (data not shown).

Images were scored for catheter position and visibility (*Table 5*). All three image guidance techniques provided equivalent confidence to operator that catheter was inside targeted chamber or vessel. Pressure measurements were necessary to confirm wedge position in all three approaches, as expected. Unlike X-ray, pressure measurements were not necessary to confirm passage from the right ventricle into the main pulmonary artery under MRI, although this advantage is not clinically important.

Catheter tip and shaft were always visible under X-ray, whereas MRI provided inferior visibility because only the tip was ever visible. Gadolinium-filled balloons were more consistently conspicuous than air-filled balloons under MRI (*Figures 2* and *3*; Supplementary material online, *Video*). Moreover, gadolinium-filled balloons could be selectively visualized using a 'saturation preparation' MRI mode that specifically enhanced the appearance of gadolinium inside the catheter tip (*Figure 3*; Supplementary material online, *Video*). Occasionally, the artefact created by the air-filled balloon was indistinguishable from other non-specific susceptibility artefacts (*Figure 4*).

Cardiac MRI findings are summarized in *Table 2*. Eight of 16 subjects had enlarged main pulmonary arteries defined as ratio of pulmonary artery to aorta diameter ratio ≥0.9.

Workflow and technique

Preparation for magnetic resonance imaging catheterization required 13.8 ± 4.7 min for the transfer from the X-ray system to the MRI system (which included placing MRI surface coils and monitoring leads), followed by 27.7 ± 6.9 min for baseline MRI scanning. The total time inside the MRI system was 68.1 ± 21.6 min.
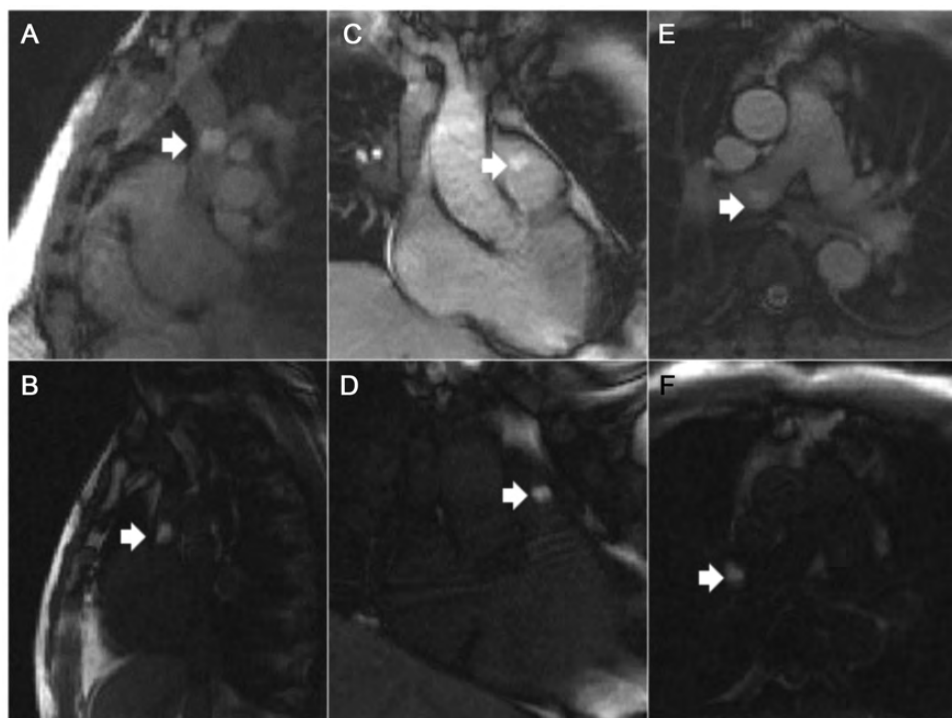
Figure 3 Magnetic resonance imaging catheterization using a gadolinium-filled balloon catheter and interactive saturation-preparation imaging. Interactive application of saturation-preparation real-time magnetic resonance imaging mode helped to highlight the appearance of the gadolinium-filled balloon. The top row indicates the normal mode, and the bottom row indicates the saturation-preparation mode. White arrows indicate catheter tips. (*A* and *B*) Superior vena cava. (*C* and *D*) Entering the main pulmonary artery from the right ventricle. (*E* and *F*) Right pulmonary artery.

Qualitatively, the team worked slowly and deliberatively during transfer from X-ray and during baseline MRI scanning. Conversely, catheter operators worked quickly during catheter manipulation.

There was no difference between total right heart catheterization times ('sheath-to-sheath intervals') among the three approaches (X-ray 19.4 ± 11.5 min, MRI air 21.4 ± 6.0 min, MRI gadolinium 21.0 ± 8.8 min, $P = 0.347$). Catheterization time includes all manipulation, pressure recording, and sampling for oximetry and therefore is longer than fluoroscopy time. MRI catheter times were not affected by which catheter came first. Procedure steps became faster with practice (*Table 6*). We attribute this to workflow enhancements in this early experience, such as consistent operating procedures, scan plane layouts, and better audio headset discipline.

Discussion

In this feasibility study, we show that MRI-guided catheterization may offer a radiation-free alternative to the current clinical practice for comprehensive transfemoral right heart catheterization. This is the first experience of comprehensive right heart catheterization (sampling both cavae and both pulmonary artery branches) performed entirely using MRI guidance in an unselected cohort of subjects, and the only paired comparison of X-ray and MRI catheterization in the same subjects. Fifteen of 16 transfemoral

catheterizations were successful without a guidewire even though most had pulmonary artery hypertension, a marker of procedural difficulty. Catheterization performance times and guidewire-free success rates were comparable to X-ray, even though MRI visualized only the tips of commercially available catheters. Indeed, there was a trend for certain procedure steps (engagement of the left pulmonary artery) to be quicker using MRI guidance. We found gadolinium-filled balloon catheters to be more conspicuous and allowed faster navigation, and therefore were more effective than air-filled balloon catheters. Finally, we found the time to perform transfemoral MRI catheterization (apart from baseline imaging) to be comparable with X-ray catheterization because of the superior chamber visualization, and without ionizing radiation. Moderate sedation appeared uneventful. The procedure has become sufficiently routine that an MRI technologist, not a physicist, operates the scanner during catheterization.

Less-routine MRI catheterization has been reported previously by other groups. Razavi *et al.*[5] from King's College in London reported 16 subjects, mostly paediatric, with congenital heart disease in whom MRI-only catheterization was successful in two and partial-MRI catheterization was successful in 14. In one follow-on report from the same group,[6] 5 of 20 similar subjects underwent MRI-only catheterization and the rest combined X-ray and MRI catheterization. In another,[7] 9 of 17 children or adults with

Table 2 **Catheterization and magnetic resonance imaging findings**

Pressures (mmHg)

	HR	SVC MBP	IVC MBP	RA MBP	RA v-wave	RV SBP	RV DBP	MPA SBP	MPA DBP	MPA MBP
AX	71.7 ± 12.5	11.7 ± 4.3	10.1 ± 4.9	10.4 ± 4.9	12.8 ± 5.3	45.7 ± 20.3	10.4 ± 5.1	43.9 ± 20.8	19.8 ± 7.4	27.9 ± 11.6
MRI-Air	69.1 ± 11.4	9.8 ± 4.3	8.9 ± 4.2	9.1 ± 3.6	11.0 ± 3.9	42.1 ± 19.6	9.3 ± 4.5	40.9 ± 20.1	18.3 ± 7.5	25.1 ± 11.3
MRI-Gd	69.7 ± 11.8	9.0 ± 3.5	8.5 ± 3.7	8.5 ± 3.6	10.8 ± 4.0	41.9 ± 19.8	8.8 ± 4.2	41.7 ± 20.5	18.9 ± 8.7	25.7 ± 12.4
P-value	0.067	0.004	0.024	0.071	0.105	0.018	0.132	0.041	0.42	0.063
	RPA SBP	RPA DBP	RPA MBP	RPA wedge	RPA wedge v-wave	LPA SBP	LPA SBP	LPA MBP	LPA wedge	
AX	38.9 ± 7.2	18.5 ± 4.5	24.9 ± 4.0	15.2 ± 4.9	18.1 ± 6.1	37.6 ± 6.5	15.8 ± 1.9	23.0 ± 2.8	11.4 ± 1.8	
MRI-Air	34.4 ± 4.3	16.4 ± 3.6	22.1 ± 2.8	13.2 ± 3.9	15.9 ± 4.9	32.8 ± 2.6	15.2 ± 2.3	21.2 ± 2.4	12.0 ± 1.7	
MRI-Gd	33.1 ± 5.2	16.4 ± 3.7	20.9 ± 3.9	13.0 ± 4.5	15.0 ± 5.9	34.4 ± 2.2	16.6 ± 3.8	21.2 ± 2.8	11.4 ± 2.6	
P-value	0.001	0.043	0.001	0.128	0.023	0.135	0.444	0.494	0.486	

Saturations (% oxyhaemoglobin)

	SVC	IVC	RA	MPA	RPA	LPA	FA
AX	68.3 ± 6.0	72.0 ± 5.3	70.0 ± 5.9	70.0 ± 6.9	73.9 ± 8.7	74.3 ± 8.5	94.0 ± 3.6
MRI-Air	59.4 ± 20.2	69.5 ± 14.7	69.9 ± 5.5	69.6 ± 5.6	72.6 ± 9.3	74.3 ± 8.8	95.3 ± 2.0
MRI-Gd	64.8 ± 15.2	68.8 ± 14.6	71.9 ± 8.1	68.9 ± 7.4	72.5 ± 9.6	73.0 ± 11.4	95.6 ± 1.8
P-value	0.264	0.612	0.607	0.338	0.032	0.854	0.545

MRI chamber size and function (mm)

Left ventricle	LV EDV	LV ESV	LV SV	LV EF
	104.2 ± 50.8	46.7 ± 40.4	57.4 ± 17.3	0.59 ± 0.11
Right ventricle	RV EDV	RV ESD	RV SV	RV EF
	118.4 ± 36.5	62.0 ± 26.0	56.4 ± 20.4	0.49 ± 0.13
Other	Aorta	MPA	LA	RA
	30.9 ± 4.0	28.9 ± 3.8	59.6 ± 7.3	53.7 ± 10.8

These are the results of pressure and oximetry measurements, compared using non-parametric methods. Pressures are statistically different but not clinically different, attributed to the diuretic effect of iodinated contrast, and are reported as not different. Saturations are the same. Chamber measurements are in millimetre. HR, heart rate; MBP, mean blood pressure; SBP, systolic blood pressure; DBP, diastolic blood pressure; SVC, superior vena cava; IVC, inferior vena cava; RA, right atrium; RV, right ventricle; MPA, main pulmonary artery; RPA, right pulmonary artery; LPA, left pulmonary artery; LV, left ventricle; EDV, end diastolic volume; ESV, end systolic volume; EF, ejection fraction; RV, right ventricle; LA, left atrium.

pulmonary artery hypertension underwent MRI-only catheteriza-tion. More recently,[8] this team reported the first two human MRI-only pulmonary valvuloplasty procedures.

Kuehne *et al.*[9] reported 12 subjects with patent foramen ovale or pulmonary artery hypertension in whom MRI-only was used to guide transfemoral balloon flotation catheters only into the right ventricle for physiology experiments; complete MRI catheter-ization was not performed. In 15 subsequent subjects,[10] MRI-only was used to guide transfemoral balloon flotation catheters only into the right atrium, right ventricle, and main pulmonary artery.

Table 3 Success of each procedural step by the image-guidance technique

Chamber	Technique	Success (%)	P-value
SVC	X-ray	93	0.368
n = 15	MRI-Air	87	
	MRI-Gd	100	
MPA	X-ray	100	1
n = 14	MRI-Air	100	
	MRI-Gd	100	
RPA	X-ray	93	0.368
n = 14	MRI-Air	86	
	MRI-Gd	93	
LPA	X-ray	77	0.030
n = 13	MRI-Air	46	
	MRI-Gd	85	
RPAW	X-ray	100	0.368
n = 12	MRI-Air	32	
	MRI-Gd	100	
LPAW	X-ray	89	0.174
n = 9	MRI-Air	67	
	MRI-Gd	100	

The step is described as entry into the specified chamber. P-values reflect a comparison of all three techniques.
MRI-Air, MRI using air-filled balloon catheter; MRI-Gd, MRI using gadolinium-filled balloon catheter; SVC, entering superior vena cava from right atrium; MPA, entering main pulmonary artery from right ventricle; RPA, entering right pulmonary artery from main pulmonary artery; LPA, entering left pulmonary artery from main pulmonary artery; RPAW and LPAW, right and left pulmonary artery wedge, respectively.

They did not steer into the superior vena cava or into the branch pulmonary arteries. Complete MRI catheterization was not performed but they used MRI flow measurement combined with catheters to assess pulmonary vascular resistance in response to a haemodynamic provocation.

Magnetic resonance imaging catheterization is not offered at present in patients ineligible for MRI because of metal in high risk locations (for example certain intracranial implants) and because of conductive implants such as pacemakers and defibrilla-tors. New devices and techniques are under development.[11] Several candidates declined to participate in this study, usually an-ticipating claustrophobia that was mitigated in participants by mod-erate sedation. The chief reasons for failure once MRI catheterization was undertaken are (i) catheter shaft kinking, detected in two subjects by tactile and visual cues and (ii) lack of a guidewire to enhance the stiffness of our passive catheters in patients with challenging anatomy or physiology. Indeed, we have long asserted the need for combined tip and shaft visualization during MRI catheterization and are working towards a safe and conspicuous ('active') MRI guidewire to impart these characteris-tics[12] and speed the procedure. Such tools are critical for novel MRI-guided interventional procedures.

Radiation exposure from X-ray guided catheterization confers a risk of malignancy that is presumed trivial in simple adult proce-dures but non-trivial in prolonged or repeated procedures espe-cially in children. Indeed DNA damage is evident after X-ray paediatric catheterization.[13,14]

Limitations of this work include extra time required for baseline MRI before catheterization, albeit to provide information not at-tainable using X-ray alone. We cannot exclude the possibility that gadolinium fluid-filled balloon catheters outperformed air-filled balloon catheters in part because of different buoyancy. Fluid-filled balloon catheters deflate adequately albeit more slowly than gas-filled ones. Missing data (from unsuccessful air-filled MRI cathe-ters) biased timing comparisons in favour of X-ray, an appropriate-ly conservative analysis strategy. We systematically performed X-ray before MRI catheterization (out of clinical priority), which may bias the comparison in favour of MRI. We believe that the clear MRI depiction of target structures obviates the value of ex-perience from the preceding X-ray procedure. Magnetic resonance imaging provides an inherent advantage in showing the location of target chambers, and an inherent disadvantage in failing to depict

Table 4 Median time to complete each procedural step with the different image-guidance modalities, in seconds (first quartile–third quartile)

	X-ray	MRI-Air	MRI-Gd	n	P-value
SVC	37.5 (14.8−76.5)	31.5 (8.3−61.8)	30.0 (6.3−60.8)	12	0.517
MPA	29.5 (11.0−50.5)	30.5 (19.8−101.0)	21.5 (13.8−88.5)	14	0.395
RPA	7.0 (4.0−44.5)	6.0 (4.3−7.0)	10.5 (3.8−26.5)	12	0.161
LPA	32.0 (10.0−67.5)	88.0 (24.5−152.0)	16.0 (14.0−33.5)*	5	0.074

MRI-Air, MRI using air-filled balloon catheter; MRI-Gd, MRI using gadolinium-filled balloon catheter; SVC, entering superior vena cava from right atrium; MPA, entering main pulmonary artery from right ventricle; RPA, entering right pulmonary artery from main pulmonary artery; LPA, entering left pulmonary artery from main pulmonary artery.
*P = 0.028 vs. X-ray.

Table 5 Catheter visibility

Chamber	Anatomic confidence score				Friedman	Tip and shaft visibility score				Friedman	Wilcoxon Gd-vs.-Air
	X-ray	MR-Air	MR-Gd	n	P-value	X-ray	MR-Air	MR-Gd	n	P-value	
SVC	1.9	1.9	2.0	12	0.607	3.0	0.9	2.0	12	<0.001	0.004
IVC	2.0	1.9	2.0	14	0.368	3.0	1.0	2.0	12	<0.001	0.002
RA	1.9	1.9	1.9	15	0.779	3.0	0.6	1.4	15	<0.001	0.001
RV	1.4	1.8	1.9	14	0.029	3.0	0.5	1.6	14	<0.001	0.001
MPA	1.9	1.6	2.0	14	0.015	3.0	0.7	1.9	14	<0.001	0.001
RPA	2.0	1.6	2.0	12	0.018	3.0	0.8	1.8	12	<0.001	0.006
RPAW	1.4	1.1	1.2	12	0.061	2.9	0.5	1.4	12	<0.001	0.009
LPA	2.0	1.7	2.0	6	0.135	3.0	0.8	1.8	6	0.004	0.038
LPAW	1.4	1.2	1.2	5	0.368	3.0	0.8	1.8	5	0.008	0.038

The left panel indicates operator confidence that the catheter is inside the targeted chamber based on imaging alone, among all three approaches. A score of 0 indicates uncertainty; 1 indicates that pressure or X-ray biplane is necessary; 2 indicates confidence that the catheter is inside the target chamber. Both MRI techniques provided equivalent operator confidence about catheter anatomic position compared with X-ray. The right panel indicates visibility of the tip and shaft of the catheter. A score of 0 indicates the tip is sometimes not located; 1 indicates the tip is mostly visible or easily located; 2 indicates the tip is visible at all times; 3 indicates the tip and shaft are visible at all times. X-ray was superior to both MRI techniques. Gadolinium-filled balloons are mostly superior to air-filled balloons.
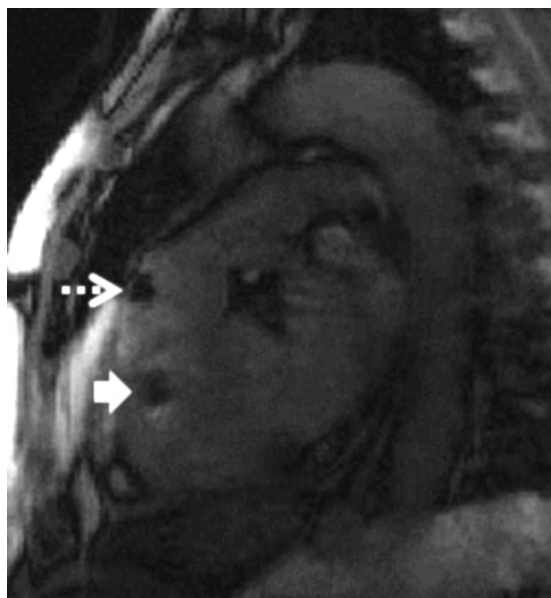

Figure 4 Ambiguity using air-filled balloon catheters. The black signal void created by air-filled balloon catheters (dashed arrow) was occasionally indistinguishable from signal voids created by other imaging artefacts (solid arrow).

the catheter shaft. Our observations about the success rate and the time to enter specific chambers are based on a small number of subjects in a feasibility study, and these results should therefore be viewed with caution.

The chief obstacle to adoption of MRI catheterization is the unavailability of conspicuous and safe catheter devices.[11] Steel, a ubiquitous component of catheter and guidewire tools because of its low cost and versatility, distorts MR images. Alternative MRI-compatible metals are available, such as cobalt−chromium used in newer stents and stent-valves, nitinol used in guidewires and cardiac occluder devices, and platinum−iridium used in coarctation stents. Removing ferrous components renders catheter tools difficult to visualize during MRI. We believe this can be addressed using 'active' MRI catheters which also serve as antennas connected to the MRI scanner. Moreover, long conductive structures, even MRI-compatible metals such as nitinol, tend to heat during MRI. We believe this can be addressed using electronic design and altered MRI techniques. Most MRI system manufacturers offer real-time MRI options sufficient to guide MRI catheterization described in this paper. However, there remains limited commercial interest in manufacturing 'active' MRI catheter devices at this early stage. Therefore our laboratory is building such tools[12] for clinical research.

This work begins translation of cardiovascular interventional MRI into clinical practice, taking advantage of superb MRI tissue visualization instead of X-rays or even direct surgical exposure. At present this comes at the expense of logistical complexity, reduced temporal and spatial resolution, and the limited range of suitable catheter devices. New transcatheter alternatives to surgery might be one justification for these challenges;[15,16] interactive visualization of ablation lesions[17] might be another. Avoiding radiation exposure, especially in children, might be still another. Our next clinical research step is to perform routine radiation-free diagnostic right and non-coronary left heart catheterization in children and in adults using active guidewires and passive catheters. We do not believe coronary artery interventional procedures are a realistic possibility because of inadequate spatial and temporal resolution. However, we do believe structural heart interventions to be realistic therapeutic targets, including delivery and repair of cardiac valve devices, non-surgical access and closure of large transthoracic cardiac access ports, repair of other cardiac structural defects, and enhanced image guidance of peripheral artery

Table 6 Learning curve

	X-ray fluoroscopy total (min)	X-ray fluoroscopy for R heart cath (min)	Transfer into MRI (min)	MRI localizers (min)	MRI total including cath (min)	X-ray catheter time (min)	MRI-air catheter time (min)	MRI-Gad catheter time (min)
First eight subjects	11.4 ± 4.9	6.6 ± 2.5	17.3 ± 3.1	29.8 ± 3.1	87.1 ± 17.8	25.4 ± 12.0	27.6 ± 9.3	31.5 ± 9.5
Second eight subjects	13.4 ± 6.5	4.2 ± 1.3	12.0 ± 4.7	25.6 ± 7.7	53.4 ± 10.8	13.4 ± 4.0	18.9 ± 4.2	15.4 ± 1.2
P-value	0.521	0.039	0.027	0.219	0.001	0.027	0.053	0.002

Time required to perform procedure steps, comparing first and second half of subjects sequentially enrolled. Most steps became significantly faster with experience.

interventions such as recanalization of chronic occlusion. Moreover, real-time MRI electrophysiology testing and cardiac ablation therapy has begun clinical testing for cardiac rhythm disorders. That said, MRI catheterization is not ready for broad clinical adoption. With improved catheter devices and workflows, even simple MRI catheterization procedures may one day be justified.

Conclusion

In this preliminary experience, real-time MRI catheterization offers an effective, radiation-free alternative to comprehensive X-ray right catheterization. With improved tools and further optimization, it may become a realistic option.

Supplementary material

Supplementary material is available at *European Heart Journal* online.

Acknowledgements

References

1. Ratnayaka K, Faranesh AZ, Guttman MA, Kocaturk O, Saikus CE, Lederman RJ. Interventional cardiovascular magnetic resonance: still tantalizing. *J Cardiovasc Magn Reson* 2008;**10**:62.
2. Sorensen TS, Atkinson D, Schaeffter T, Hansen MS. Real-time reconstruction of sensitivity encoded radial magnetic resonance imaging using a graphics processing unit. *IEEE Trans Med Imaging* 2009;**28**:1974–1985.
3. Wu V, Barbash IM, Ratnayaka K, Saikus CE, Sonmez M, Kocaturk O, Lederman RJ, Faranesh AZ. Adaptive noise cancellation to suppress electrocardiography artifacts during real-time interventional MRI. *J Magn Reson Imaging* 2011;**33**: 1184–1193.
4. Breuer FA, Kellman P, Griswold MA, Jakob PM. Dynamic autocalibrated parallel imaging using temporal GRAPPA (TGRAPPA). *Magn Reson Med* 2005;**53**: 981–985.
5. Razavi R, Hill DL, Keevil SF, Miquel ME, Muthurangu V, Hegde S, Rhode K, Barnett M, van Vaals J, Hawkes DJ, Baker E. Cardiac catheterisation guided by MRI in children and adults with congenital heart disease. *Lancet* 2003;**362**: 1877–1882.
6. Miquel ME, Hegde S, Muthurangu V, Corcoran BJ, Keevil SF, Hill DL, Razavi RS. Visualization and tracking of an inflatable balloon catheter using SSFP in a flow phantom and in the heart and great vessels of patients. *Magn Reson Med* 2004; **51**:988–995.
7. Muthurangu V, Atkinson D, Sermesant M, Miquel ME, Hegde S, Johnson R, Andriantsimiavona R, Taylor AM, Baker E, Tulloh R, Hill D, Razavi RS.

Measurement of total pulmonary arterial compliance using invasive pressure monitoring and MR flow quantification during MR-guided cardiac catheterization. *Am J Physiol Heart Circ Physiol* 2005;**289**:H1301–H1306.

8. Tzifa A, Krombach GA, Kramer N, Kruger S, Schutte A, von Walter M, Schaeffter T, Qureshi S, Krasemann T, Rosenthal E, Schwartz CA, Varma G, Buhl A, Kohlmeier A, Bucker A, Gunther RW, Razavi R. Magnetic resonance-guided cardiac interventions using magnetic resonance-compatible devices: a pre-clinical study and first-in-man congenital interventions. *Circ Cardiovasc Interv* 2010; **3**:585–592.

9. Kuehne T, Yilmaz S, Steendijk P, Moore P, Groenink M, Saaed M, Weber O, Higgins CB, Ewert P, Fleck E, Nagel E, Schulze-Neick I, Lange P. Magnetic resonance imaging analysis of right ventricular pressure-volume loops: *in vivo* validation and clinical application in patients with pulmonary hypertension. *Circulation* 2004; **110**:2010–2016.

10. Kuehne T, Yilmaz S, Schulze-Neick I, Wellnhofer E, Ewert P, Nagel E, Lange P. Magnetic resonance imaging guided catheterisation for assessment of pulmonary vascular resistance: *in vivo* validation and clinical application in patients with pulmonary hypertension. *Heart* 2005;**91**:1064–1069.

11. Saikus CE, Lederman RJ. Interventional cardiovascular magnetic resonance imaging: a new opportunity for image-guided interventions. *JACC Cardiovasc Imaging* 2009;**2**:1321–1331.

12. Sonmez M, Saikus CE, Bell JA, Franson DN, Halabi M, Faranesh AZ, Ozturk C, Lederman RJ, Kocaturk O. MRI active guidewire with an embedded temperature probe and providing a distinct tip signal to enhance clinical safety. *J Cardiovasc Magn Reson* 2012. Advance Access published 21 June 2012, doi:10.1186/1532-429X-14-38.

13. Beels L, Bacher K, De Wolf D, Werbrouck J, Thierens H. Gamma-H2AX foci as a biomarker for patient X-ray exposure in pediatric cardiac catheterization: are we underestimating radiation risks? *Circulation* 2009;**120**:1903–1909.

14. Ait-Ali L, Andreassi MG, Foffa I, Spadoni I, Vano E, Picano E. Cumulative patient effective dose and acute radiation-induced chromosomal DNA damage in children with congenital heart disease. *Heart* 2010;**96**:269–274.

15. Barbash IM, Saikus CE, Faranesh AZ, Ratnayaka K, Kocaturk O, Chen MY, Bell JA, Virmani R, Schenke WH, Hansen MS, Slack MC, Lederman RJ. Direct percutaneous left ventricular access and port closure pre-clinical feasibility. *JACC Cardiovasc Interv* 2011;**4**:1318–1325.

16. Ratnayaka K, Saikus CE, Faranesh AZ, Bell JA, Barbash IM, Kocaturk O, Reyes CA, Sonmez M, Schenke WH, Wright VJ, Hansen MS, Slack MC, Lederman RJ. Closed-chest transthoracic magnetic resonance imaging-guided ventricular septal defect closure in swine. *JACC. Cardiovasc Interv* 2011;**4**:1326–1334.

17. Kolandaivelu A, Zviman MM, Castro V, Lardo AC, Berger RD, Halperin HR. Non-invasive assessment of tissue heating during cardiac radiofrequency ablation using MRI thermography. *Circ Arrhythm Electrophysiol* 2010;**3**:521–529.